AFFDL-TR-66-153
PART II

THE DEVELOPMENT AND EVALUATION OF THE CAL/AIR FORCE DYNAMIC WIND-TUNNEL TESTING SYSTEM

PART II — DYNAMIC TESTS OF AN F-104 MODEL

IRVING C. STATLER

CORNELL AERONAUTICAL LABORATORY, INC.

FOREWORD

The research effort documented in this report was performed for the Air Force Flight Dynamics Laboratory (AFFDL), Research and Technology Division, Wright-Patterson Air Force Base, Ohio by the Applied Mechanics Department of the Cornell Aeronautical Laboratory, Inc. (CAL), Buffalo, New York. This work was done under Air Force Contract AF 33(616)-8034.

The project engineer from AFFDL for this program was Mr. Jerry Jenkins of the Control Criteria Branch, Flight Control Division. The F-104 model and its unusual dummy model and balance system were designed by Mr. Donald W. Young of the Experimental Facilities Instrumentation Branch, Flight Mechanics Division, AFFDL.

At CAL, Dr. Irving C. Statler, Head of the Applied Mechanics Department, was the principal investigator. Messrs. Orren B. Tufts and Walter J. Hirtreiter, Principal Engineers in the Applied Mechanics Department, shared the project engineering responsibilities and were ably aided by Mr. George Jackson, Engineering Assistant.

Part I of this report describes the equipment and the evaluation tests performed with an F-80 model. Part II presents only the results of additional evaluation tests with an F-104 model.

This technical report has been reviewed and is approved.

C. B. Westbrook

C. B. WESTBROOK
Chief, Control Criteria Branch
Flight Control Division
Air Force Flight Dynamics Laboratory

ABSTRACT

The development of a new technique for dynamic testing in wind tunnels and evaluation tests of the system with an F-80 model were described in Part I of this report. Although those tests adequately demonstrated the unusual capabilities of this dynamic testing system, the F-80 model was limited to subsonic speeds. This part of the report (Part II) describes an additional series of evaluation tests that were performed with a model of an F-104 airplane. The model had been designed and fabricated by the Air Force Flight Dynamics Laboratory and incorporated an unusual force and motion sensing system utilizing an internal dummy model with duplicate mass, inertia, and c.g. location. Longitudinal dynamic tests were performed with this model up through the transonic speed range. The results are evaluated with respect to the operation of the dynamic testing system and to the performance of the dummy model for measuring motion and canceling inertial loads.

TABLE OF CONTENTS

ILLUSTRATIONS

TABLES

SYMBOLS

$\underline{\textcircled{A}}$ is the readout indication of the angular acceleration, $\underline{\textcircled{A}} \equiv -(\underline{D}_A + K_1 \underline{D}_F)$, rad/sec.^{2}

C_{L_α} is the slope of the lift-coefficient curve. (Dynamically it is given by the magnitude of the component of $\underline{\textcircled{F}}$ normal to $\tau \underline{\textcircled{A}}/2\pi j$ divided by $qS(\tau/2\pi)^2 |\underline{\textcircled{A}}|$ in rotation or by the magnitude of the component of $\underline{\textcircled{F}}$ normal to $\underline{\textcircled{L}}/U$ divided by $qS(\tau/2\pi)(|\underline{\textcircled{L}}|/U)$ in plunging.)

C_{m_α} is the slope of the moment-coefficient curve. (Dynamically it is given by the magnitude of the component of $\underline{\textcircled{M}}$ normal to $\tau \underline{\textcircled{A}}/2\pi j$ divided by $qSc(\tau/2\pi)^2 |\underline{\textcircled{A}}|$ in rotation or by the magnitude of the component of $\underline{\textcircled{M}}$ normal to $\underline{\textcircled{L}}/U$ divided by $qSc(\tau/2\pi)(|\underline{\textcircled{L}}|/U)$ in plunging.)

$C_{L_{\dot\alpha}}$ is the derivative of the lift coefficient with respect to rate of change of angle of attack, 1/rad/sec.

$C_{m_{\dot\alpha}}$ is the derivative of the moment coefficient with respect to rate of change of angle of attack, 1/rad/sec.

$C_{L_{\dot\theta}}$ is the derivative of the lift coefficient with respect to pitching velocity, 1/rad/sec.

$C_{m_{\dot\theta}}$ is the derivative of the moment coefficient with respect to pitching velocity, 1/rad/sec.

c is the mean aerodynamic chord, ft.

$c.g.$ is the center of gravity

$\underline{D}_A$ is the signal from the aft strain-gage bridge of the dummy model balance

$\underline{D}_F$ is the signal from the forward strain-gage bridge of the dummy model balance

$\underline{\textcircled{F}}$ is the aerodynamic normal force, $\underline{\textcircled{F}} \equiv \underline{M}_F - W_M^* \underline{D}_F$, lb. (positive up)

g is the acceleration due to gravity, g = 32.2 ft/sec.^{2}

I_M is the pitching moment of inertia of the F-104 model about its c.g., lb. ft. sec.^{2}

I^* is used to cancel the moment due to inertial reaction (see Figure 6)

SYMBOLS (Cont'd)

K_1 is the product of the ratio of the sensitivities of the aft to the forward strain-gage bridges of the dummy model times the quantity (ℓ_1/ℓ_2) and is used to correct for error in location of the dummy model c. g. (see Figure 6)

K_2 is the parameter for the F-104 model corresponding to K_1 for the dummy model

$\underline{\textcircled{L}}$ is the readout indication of the linear (vertical) acceleration, $\underline{\textcircled{L}} \equiv -\underline{D}_F$, ft/sec.^{2}

ℓ_1 is the distance of the c. g. of the dummy model forward (along the longitudinal axis) from the pivot of the dummy model balance, ft.

ℓ_2 is the distance of the c. g. of the dummy model forward (along the longitudinal axis) from the sensitive axis of the dummy model's aft strain beam, ft.

$\underline{\textcircled{M}}$ is the aerodynamic pitching moment, $\underline{\textcircled{M}} \equiv \underline{M}_A + K_2\underline{M}_F - I_M^*(\underline{D}_A + K_1\underline{D}_F)$ ft. lb. (positive for model nose up)

$\underline{M}_A$ is the signal from the aft strain-gage bridge of the F-104 model balance

$\underline{M}_F$ is the signal from the forward strain-gage bridge of the F-104 model balance

M is the Mach number

q is the dynamic pressure, lb/ft.^{2}

S is the wing area, ft.^{2}

U is the free stream velocity, fps.

W_M is the weight of the F-104 model, lb.

W_M^* is used to cancel the normal force due to inertial reaction (see Figure 6)

$\bar{\alpha}$ is the mean angle of attack, rad. or deg.

$\underline{\alpha}$ is the oscillatory angle of attack, rad. (positive nose up relative to tangent to flight path)

SYMBOLS (Cont'd)

$\underline{\theta}$ is the oscillating rotational angle about the c.g., rad. (positive nose up relative to horizontal), $\underline{\theta} = -(\tau/2\pi)^2 \ddot{\underline{\theta}}$

$\ddot{\underline{\theta}}$ is the angular velocity of the model about its c.g., rad/sec. (positive for model nose up)

τ is the oscillation period, sec.

NOTE: An underscored symbol denotes a vector.

SECTION 1

INTRODUCTION

A complete description of the development and the operation of the CAL/Air Force Dynamic Wind-Tunnel Testing System is presented in Part I of this report. [1]* It was noted there that this unique oscillatory mounting system was developed by the Cornell Aeronautical Laboratory, Inc. (CAL) under the sponsorship of the U. S. Air Force Flight Dynamics Laboratory, Control Criteria Branch, to meet the need for wind-tunnel tests of unsteady aerodynamics, particularly in the transonic speed range. By means of this system, a model in a wind tunnel can be forced precisely in any desired planar sinusoidal motion. Also discussed in Part I of this report were the wind-tunnel tests of a model of an F-80 aircraft which were performed for purposes of evaluating the capabilities of this dynamic testing system. The versatility and overall accuracy of the dynamic testing system were demonstrated in a series of wind-tunnel tests using the F-80 model at three frequencies and four Mach numbers. These tests provided, for the first time, a complete systematic set of dynamic measurements of aerodynamic lift and pitching moment. The unusual capabilities of this dynamic testing system were demonstrated in this examination of the longitudinal dynamics of an F-80 aircraft model. These tests provided measurements of the separate components of the rotary damping moment. The moment due to rate of change of angle of attack was measured by oscillating the model in pure plunging motion. The moment due to pitch rate was measured during a pure pitching motion. A self check of the system was provided by a comparison of the sum of these two derivatives to the total rotary damping moment derivative as measured in rotation. The demonstrated ability of this system to measure the separate components of the total rotary damping moment, while important in its own right, is equally significant for its indication of the overall accuracies which have been achieved.

The F-80 model was limited, however, to testing at subsonic speeds because of buffeting, and additional investigations with the dynamic testing system to the limits of the capabilities of CAL's 8-Ft. Variable-Density Transonic Wind Tunnel were desirable. A model of an F-104 airplane was made available to CAL for this purpose by the Air Force Flight Dynamics Laboratory (AFFDL). This model and its unique internal force and motion sensing system had been designed and built at Wright-Patterson Air Force Base specifically for the purpose of performing dynamic tests in the 10-Foot Wind Tunnel which existed at Wright Field at that time. This wind tunnel was dismantled, however, prior to completion of the calibration tests of the model and its balance. It was determined at the time that, with only slight

---

* Bracketed numbers denote references.

modifications to the model and with the construction of a new forward sting, this F-104 model could be adapted for testing on the CAL/Air Force Dynamic Wind-Tunnel Testing System. This provided the opportunity for additional wind-tunnel tests with the dynamic testing system up through the transonic speed range and, also, for an evaluation of the unique force and motion sensing system contained in this F-104 model. A description of these tests and their results constitute this part of the report.

SECTION 2

THE MODEL

The 7-1/2%-scale model of the USAF F-104 fighter airplane (shown in Figure 1) is nearly 50 inches long with about a 20-inch wing span. The fuselage is molded in two sections of glass-fiber laminations impregnated with epoxy resin. Helicoil threaded inserts in the lower half fuselage permit the assembly of the upper and lower halves with machine screws. The wings and tail surfaces are exceptionally high-quality magnesium castings, which are attached by machine screws into steel fittings molded into the plastic fuselage.

Further information on the dimensions and geometry of this model is presented in Table I.

In Figure 1, the model is shown as mounted on the sting in preparation for dynamic testing. (The smooth finish on the model is evident from the highlights in this photograph.)

Assembled within the fuselage of the F-104 model is a "dummy model", as shown in Figure 2. This dummy model was constructed so that its mass, moment of inertia, and center-of-gravity location duplicate precisely those of the F-104 model. The dummy model structure is an aluminum-alloy casting to which lead ballast is bolted to obtain the desired weight, inertia and c. g. location. The dummy model and the F-104 model are attached to the sting through two identical balance systems. The dummy model is constructed in two sections (upper and lower halves) so that it can be attached to its own balance and assembled around the model's balance. The attachment of the dummy model to its balance is indicated by the bolt pattern on the top of the dummy model shown in Figure 2. The F-104 model is attached to its balance through access holes in the bottom of the dummy model, as indicated in the side view shown in Figure 3. Although obviously all the available volume has been used, sufficient space exists between the dummy and the F-104 models so that no contact is made even under aerodynamic loads.

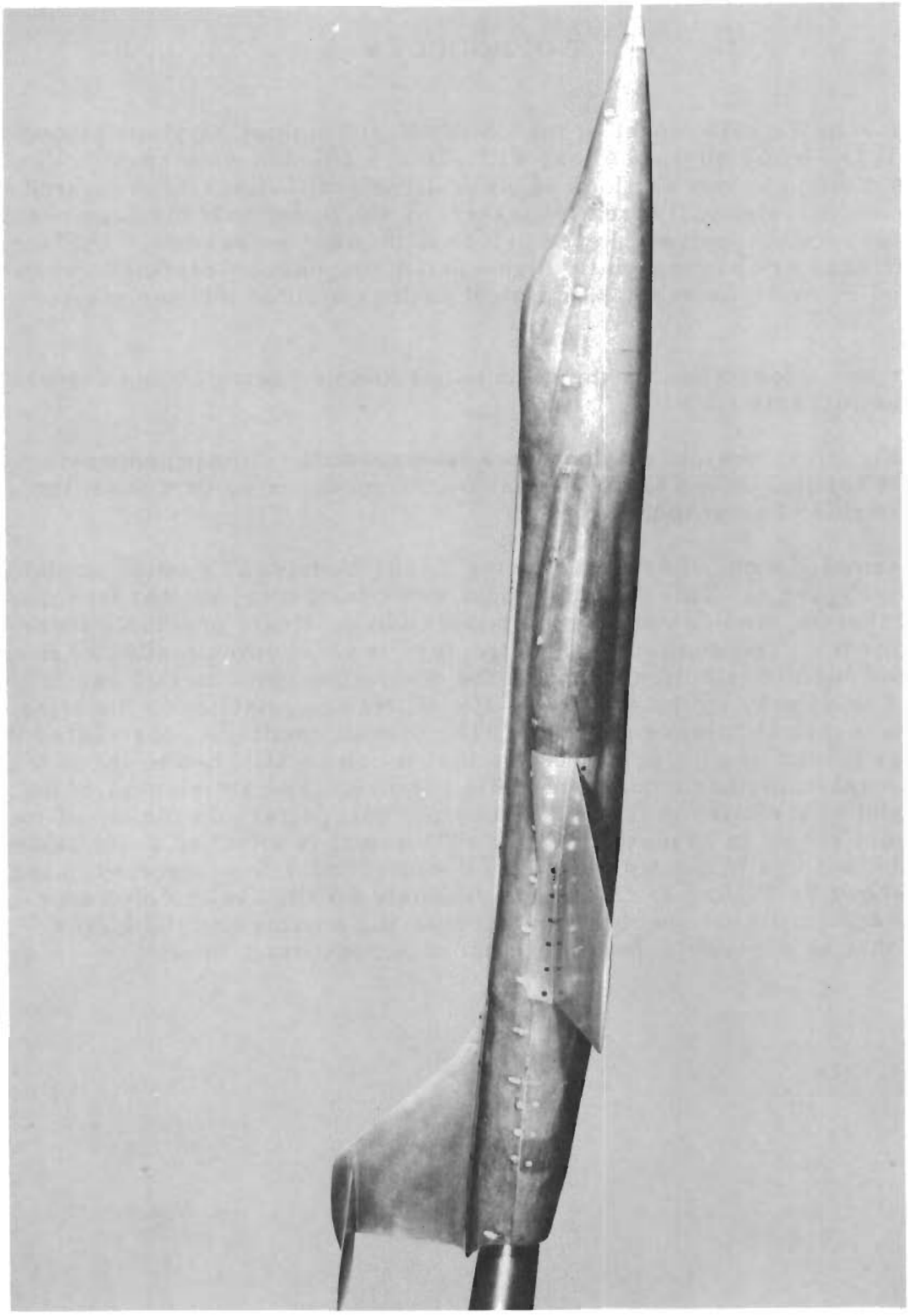

Figure 1 THE F-104 DYNAMIC TESTING MODEL

Table I

COMPARATIVE MODEL GEOMETRIES

	AIR FORCE MODEL DWG NO. 558K472	NACA RM A56I04 (REF 5)		NASA MEMO 6-5-59A (REF 3)		NACA RM A54D05 (REF 4)	
ORIGINAL SCALE	0.076	0.099		0.072		0 .086	
		ACTUAL	SCALED TO AF. MODEL	ACTUAL	SCALED TO AF. MODEL	ACTUAL	SCALED TO AF. MODEL
WING							
SPAN, b, ft	1.638	2.16	1.64	1.55	1.64	1.87	1.65
AREA, S, sq ft	1.091	1.90	1.10	0.99	1.11	1.41	1.10
MAC, c, ft	0.717	0.93	0.72	0.67	0.71	0.80	0.70
HORIZONTAL TAIL							
SPAN, b_t, ft	0.894	1.20	0.91	0.86	0.91	1.00	0.88
AREA, S_t, sq ft	0.271	0.48	0.28	——	——	0.346	0.27
MAC, c_t, ft	0.335	0.44	0.33	——	——	0.378	0.33
TAIL LENGTH, ft (25% TAIL CHORD → 25% WING CHORD)	1.384	1.67	1.27	1.19	1.26	1.43	1.26
HEIGHT, ft	0.59	0.69	0.52	0.49	0.52	0.68	0.60
TAIL LENGTH, ft (25% TAIL CHORD → 16.6% WING CHORD)	1.444	1.74	1.34	1.25	1.32	1.50	1.33
BODY							
LENGTH, B_ℓ, ft	3.88	4.65	3.54	3.29	3.48	3.77	3.33
MOMENT CENTER (ON BODY CENTER LINE) HORIZONTAL LOCATION AFT OF LEADING EDGE OF c,	16.6%	25%	16.6%	25%	16.6%	25%	16.6%

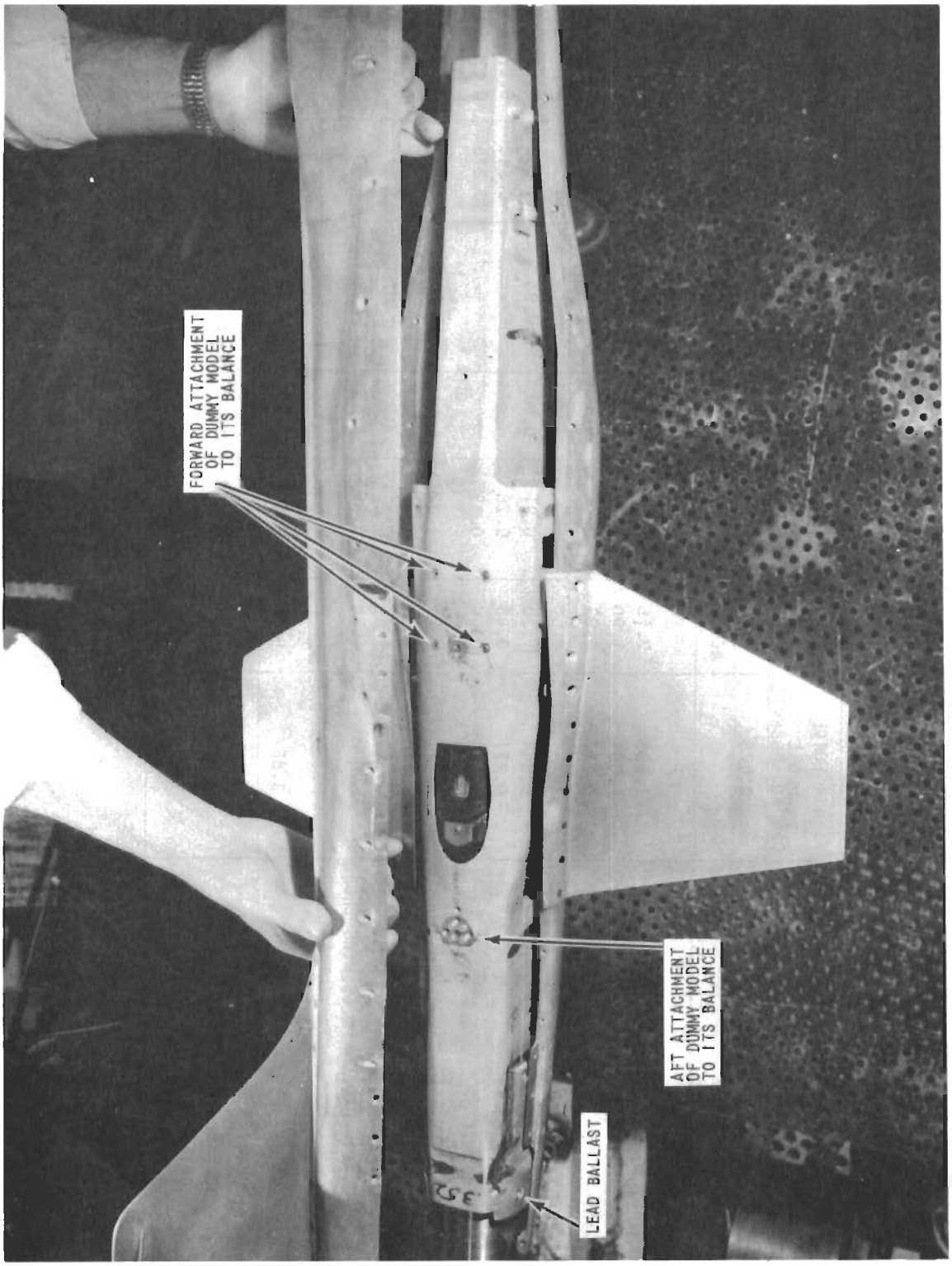

Figure 2 THE DUMMY MODEL WITHIN THE F-104 MODEL

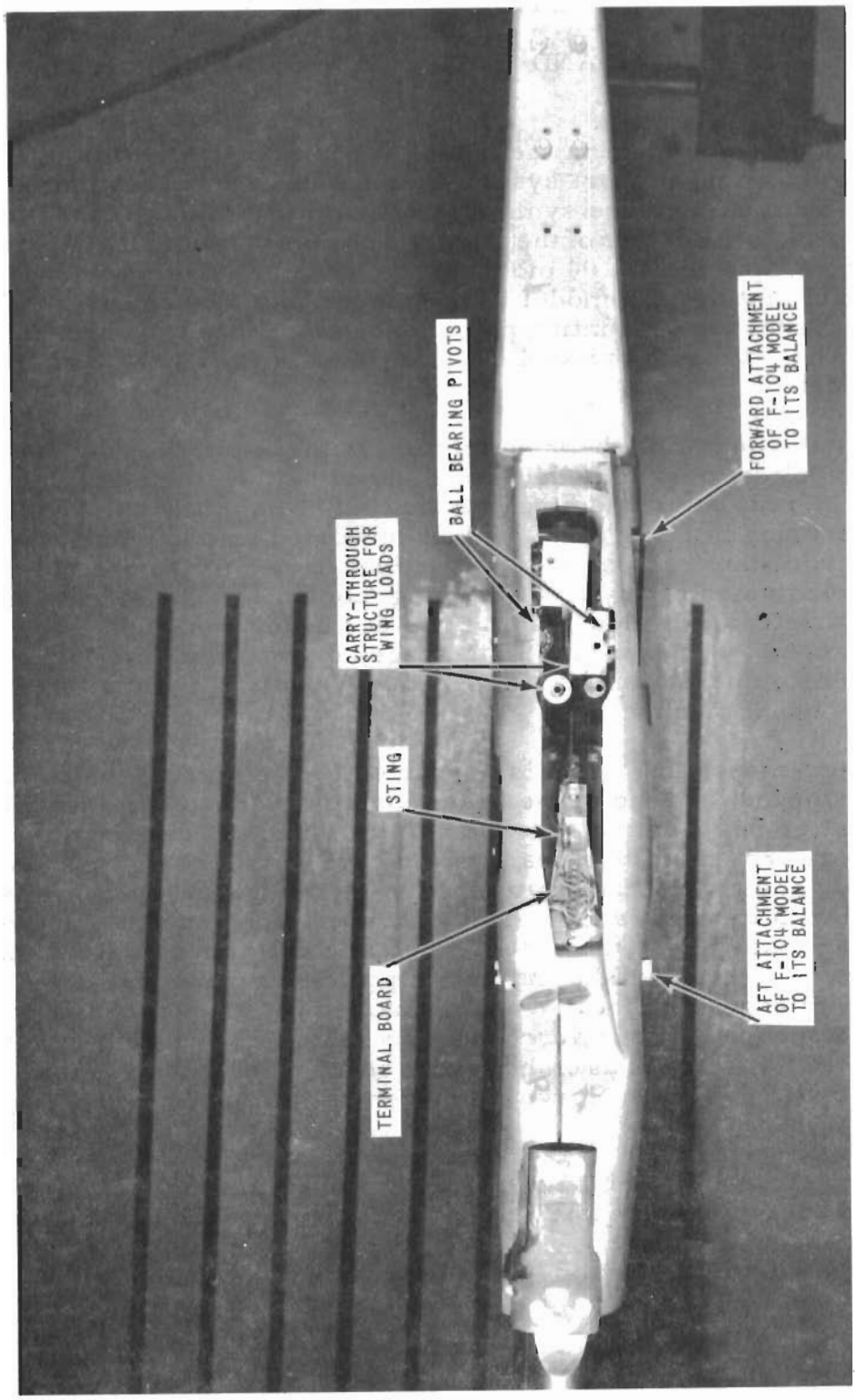

Figure 3 SIDE VIEW OF THE DUMMY MODEL

SECTION 3

THE FORCE AND MOTION SENSORS

The measurement system in the model is shown in the sketch of Figure 4. The balance and support systems for the dummy model and the F-104 model are identical and are symmetrically arranged with respect to a horizontal plane through the center of the sting. The dummy model is supported by the upper system, and the F-104 model is supported by the lower one. The aft attachment point of each model is to its moment-measuring, strain-gaged beam. At the forward mounting points, each model is attached to its balance through a ball-bearing pivot which is designed to be at the center of gravity of the model.

Except for the negligible bearing friction in these pivots, the total pitching moment applied to each model is measured by the single strain beam located at the rear attachment point about 8-1/4 in. aft of the pivot. The moment-measuring beam is a hollow box supported by two blade-like flexures which permit the transmission of vertical forces to the box but minimize the transmission of any local pitching moments. The loads are measured by the strain gages mounted on the sides of the box which are parallel to the plane of the flexures. Strain gages on the other two faces of the box provide the compensation for temperature sensitivity of the strain-gage bridge in the usual manner.

The moment-measuring beam is supported by a structure which is cantilevered from the forward end of the beam containing the shear-measuring flexures. This latter beam-flexure complex is designed to be insensitive to moments. The forward end of this beam is attached to the model through the ball-bearing pivot, and the aft end is attached to the sting. A part of this beam and aligned with its axis is a hollow, square-cross-section beam through which all the shear loads are taken out. The elastic deflection curve of this square beam is an "S" shape with an inflection point midway along its longitudinal axis. Strain gages are located at the quarter points of this beam. This strain-gaged square beam is surrounded by four flexures which act to maintain the parallelism of the ends of the square beam under loading, thereby restraining the elastic deflection curve of the central beam to an "S" shape.

All the strain gages used in the balance system are of the type ABF-32. The strain-gage bridges measuring normal force consist of four active arms for each model, whereas two of the four arms in each of the moment-measuring strain-gage bridges are effectively inactive. Each of the model balances (that for the F-104 and for the dummy) is limited to 500 in. lbs. of moment and 400 lbs. of normal force.

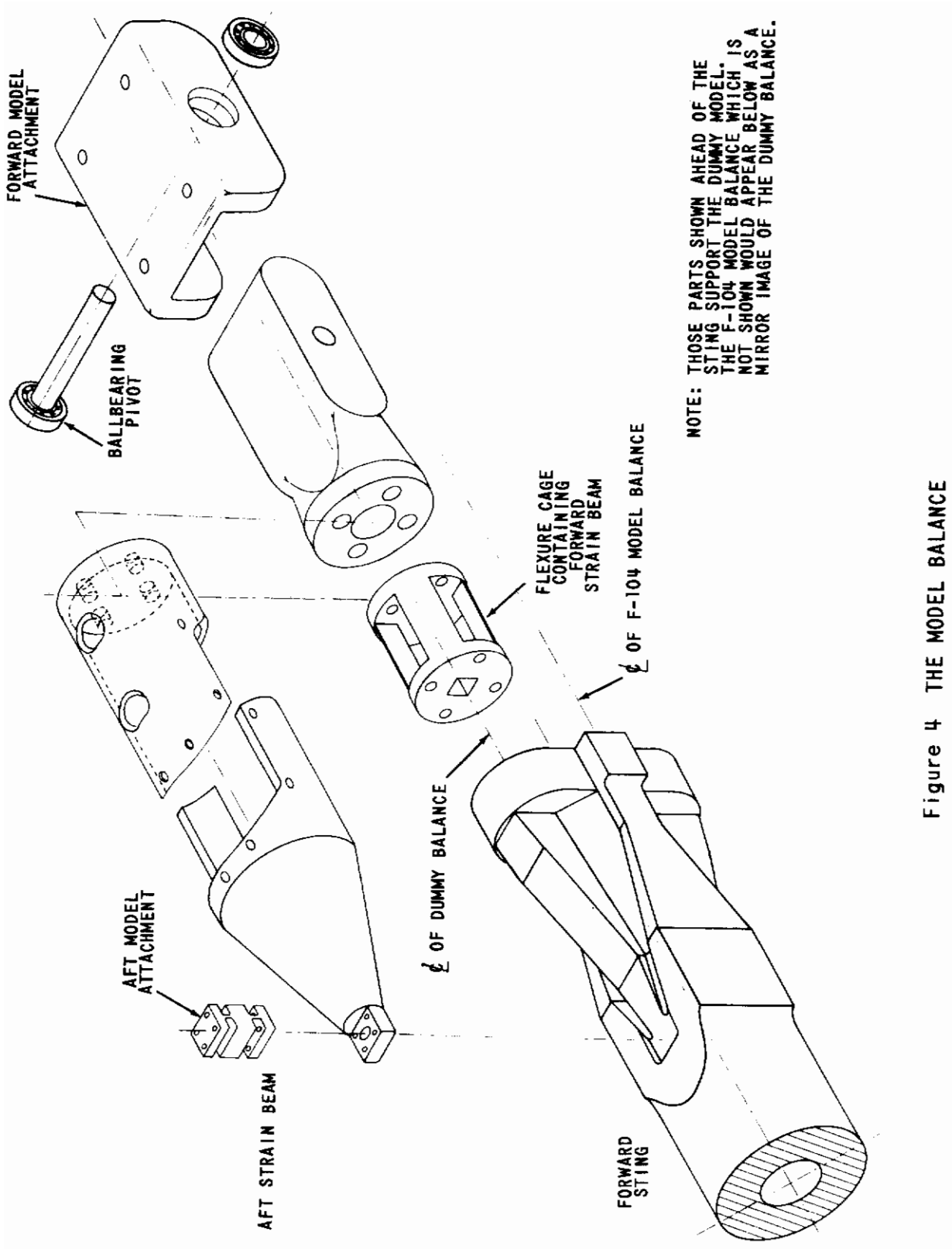

Figure 4 THE MODEL BALANCE

In the dynamic testing of the F-104 model, the dummy model replaced the linear and the angular accelerometers which constituted the motion sensors in the dynamic tests of the F-80 model [1]. After calibration, signals from the normal force portion of the dummy model balance were used as measures of the vertical acceleration of the c.g., and signals from the moment measuring portion of this balance were interpreted as measures of the angular acceleration about the c.g. Signals from the dummy model balance could also be used to cancel signals due to the inertial reaction loads from the F-104 model balance.

SECTION 4

CALIBRATION OF THE DUMMY MODEL AND THE F-104 MODEL BALANCES

The following sketch indicates the essential features of the balance system and support for both the dummy model and the F-104 model.

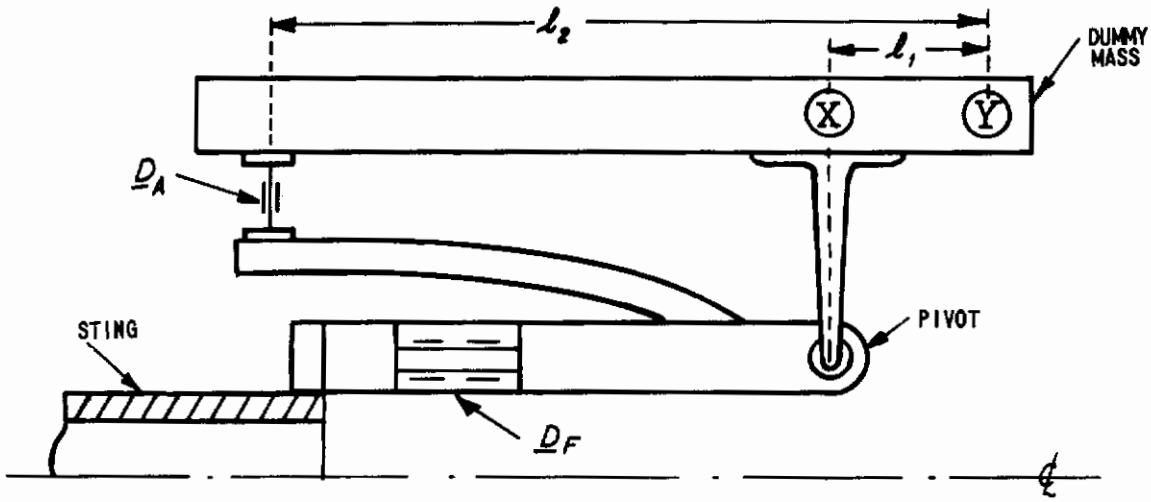

Shown here is the system for the dummy model although, as indicated previously, it is identical to the one for the F-104 model. D_A and D_F designate the signals from the aft strain-gage bridge and from the forward strain-gage bridge, respectively, of the dummy model balance. (In subsequent discussion of the F-104 model balance, the corresponding signals will be designated as M_A and M_F.) If the dummy model were balanced perfectly so that its center of gravity is located precisely at the attachment point designated as X , then the signal from the forward strain-gage bridge, D_F , would be proportional to the vertical acceleration, and the signal from the aft strain-gage bridge, D_A , would be proportional to the angular acceleration. However, if the c. g. of the dummy model is improperly located at, say, Y , then, while the signal D_F would still be proportional to the linear acceleration, the combined signal $D_A + K_1 D_F$ would now be proportional to the angular acceleration. K_1 is the product of the ratio of the sensitivities of the aft strain-gage bridge to the forward strain-gage bridge times the quantity (ℓ_1/ℓ_2) .

The following procedure was used to calibrate the dummy model balance in order to use it for measuring the vertical acceleration of its c. g. and the angular acceleration about its c. g. The dummy model was mounted on the forward sting of the mechanical oscillator in the normal manner (see Figure 5). A special platform was built which could be mounted to the same attachment points normally used for the F-104 model. This permitted an angular accelerometer and a linear accelerometer to be located very precisely with respect to the ball-bearing pivot of the dummy model balance. With the oscillator operating at about 8 cps, the four signal processing channels of the dynamic testing system (described in Reference 1) were used in a normal manner to monitor the signal from the linear accelerometer, the signal from the angular accelerometer, the forward strain-gage bridge signal, $\underline{D}_F$, and the composite signal $\underline{D}_A + K_1 \underline{D}_F$. First, a pure translational motion was set up with about 10 g's indicated by the linear accelerometer and less than 1/8 of a radian/sec.^{2} indicated by the angular accelerometer. The signals $\underline{D}_A$ and $\underline{D}_F$ were combined in the mixing unit (see Figure 6) and the quantity K_1 was adjusted until $\underline{D}_A + K_1 \underline{D}_F$ was minimized. The readout corresponding to the signal $\underline{D}_F$ was calibrated in counts/g by ratioing it to the g's indicated by the linear accelerometer.

The oscillator controls were then adjusted so that, at the same frequency of about 8 cps, a pure rotational motion was set up with about 50 radians/sec.^{2} indicated by the angular accelerometer and less than 1/4 g indicated by the linear accelerometer. (As a check of its calibration, the $\underline{D}_F$ readout should also indicate less than 1/4 g.) The $\underline{D}_A + K_1 \underline{D}_F$ readout was then calibrated in counts/radian/sec.^{2} by ratioing it to the indicated angular acceleration. (As a check of this calibration, the $\underline{D}_A + K_1 \underline{D}_F$ readout during the previous pure plunging test should have corresponded to the less than 1/8 radian/sec.^{2} indicated by the angular accelerometer.)

These calibrations of the $\underline{D}_F$ and the $\underline{D}_A + K_1 \underline{D}_F$ channels were then checked for several different combinations of linear and angular accelerations and several frequencies. In the latter case, the changes in the sensitivities of the linear and the angular accelerometers with frequency were accounted for in accordance with the calibrations reported in Reference 1.

During the course of these calibration tests, test signals were introduced to all four channels in the manner described in detail in Part I of this report [1]. These test signals provided calibrations of each of the four channels in terms of counts of readout/peak volt of input signal and enabled the conversion of the calibrations from counts/unit measured to volts/unit measured. With an excitation voltage to the strain-gage bridges of 5.27 volts, the sensitivities were determined to be 0.188 volts/g for the $\underline{D}_F$ channel and 0.0378 volts/radian/sec.^{2} for the $\underline{D}_A + K_1 \underline{D}_F$ channel and constant with frequency over the operating range.

After completing the calibration of the $\underline{D}_F$ channel to measure vertical acceleration and the $\underline{D}_A + K_1 \underline{D}_F$ channel to measure pitching acceleration, the actual linear and angular accelerometers were removed and the F-104 model was mounted on its balance in the normal manner. The calibration

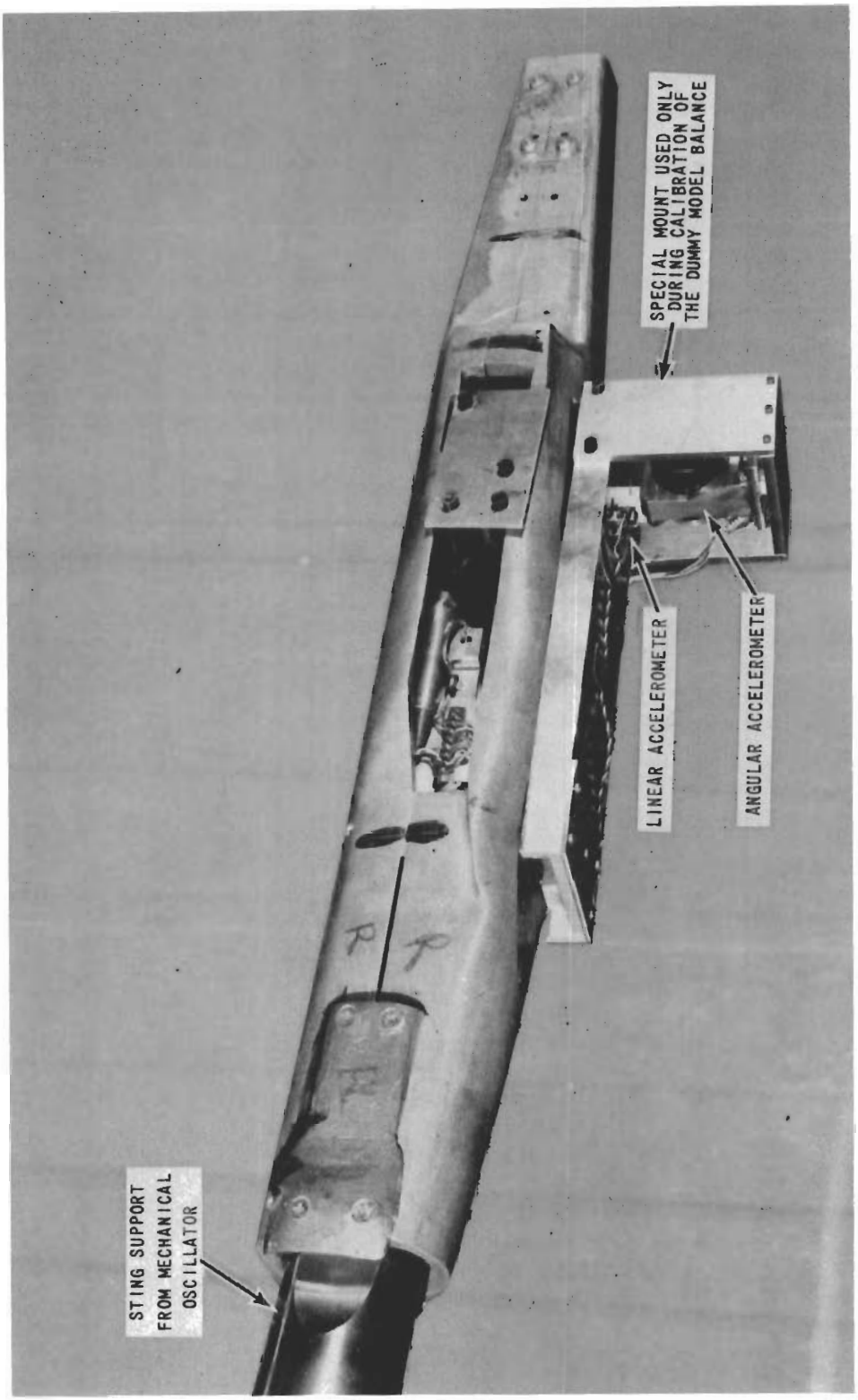

Figure 5 THE SETUP FOR CALIBRATION OF THE DUMMY MODEL BALANCE

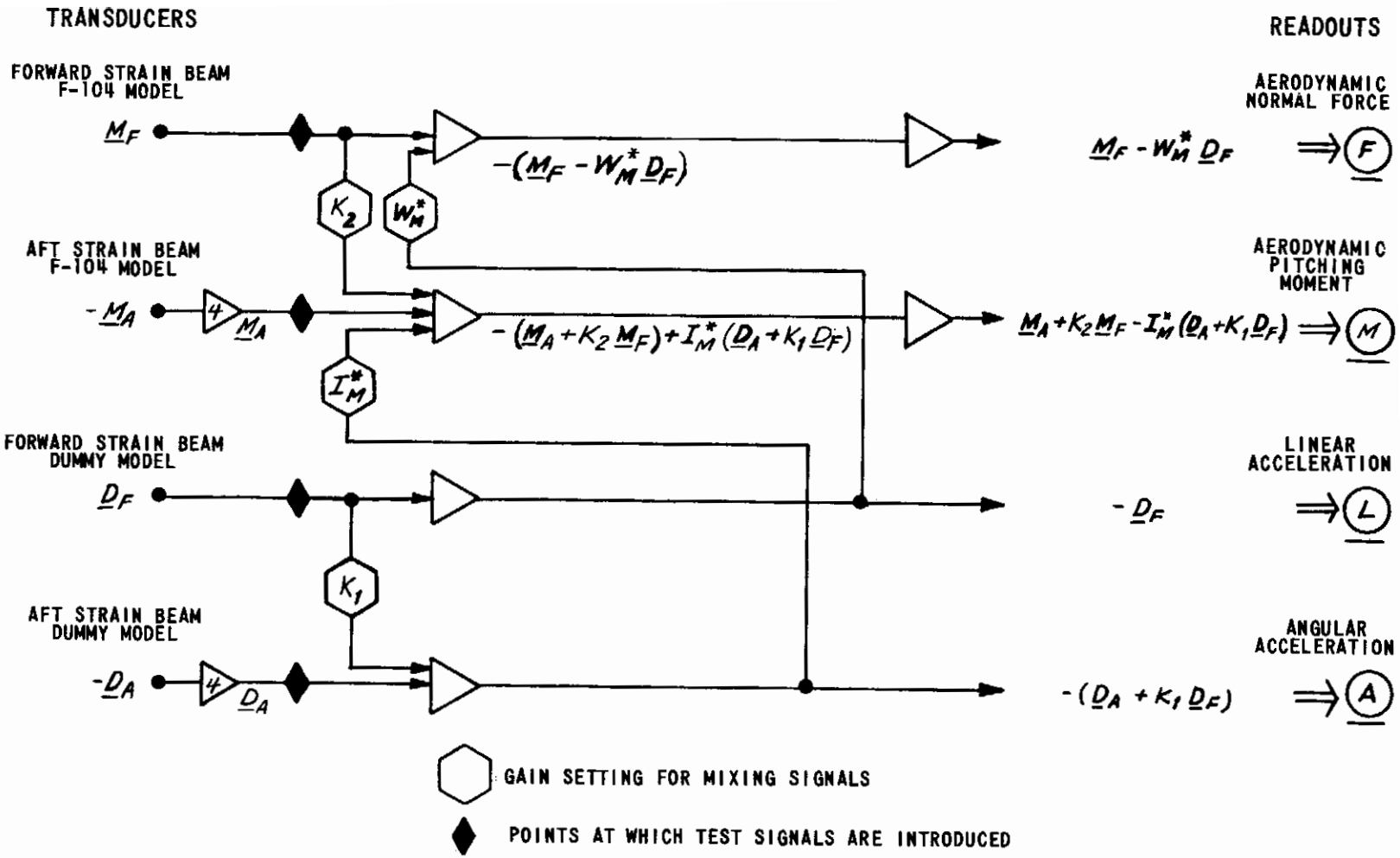

Figure 6 OPERATIONS PERFORMED IN THE SIGNAL MIXING UNIT

of the F-104 model balance proceeded in much the same manner as that of the dummy model balance. As pointed out previously, the balance systems are identical and, as in the case of the dummy model, the c.g. of the F-104 model might also be displaced from perfect alignment with the pivot of its balance. The signal from the forward strain-gage beam of the F-104 model, $\underline{M}_F$, will still be a measure of the total normal force but, as for the dummy model, a combined signal from the aft strain-gage beam and the forward strain-gage beam, $\underline{M}_A + K_2 \underline{M}_F$, is required to provide a measure of the pitching moment.

To calibrate the F-104 model balance for measurement of normal force and pitching moment, the oscillator controls were first adjusted so that, at about 8 cps, the readout $\underline{D}_A + K_1 \underline{D}_F$ indicated less than 1/8 radian/sec.^{2} of angular acceleration and the readout $\underline{D}_F$ indicated 10 g's of vertical acceleration. The quantity K_2 was adjusted in the mixing unit (see Figure 6) until the signal $\underline{M}_A + K_2 \underline{M}_F$ was minimized. (The residual signal corresponded to the pitching moments due to the small rotational motion, to the virtual mass, and to the drag on the horizontal tail when these tests were performed under other than near-vacuum conditions.) The readout corresponding to the signal $\underline{M}_F$ was calibrated in counts/lb. by ratioing it to the product of the F-104 model weight in pounds times the g's indicated by $\underline{D}_F$. In this pure plunging motion, a signal from $\underline{D}_F$ was then subtracted in the mixing unit (see Figure 6) from the $\underline{M}_F$ signal and the amount was adjusted until $\underline{M}_F - W_M^* \underline{D}_F = 0$ (to within the normal force due to apparent mass and wing and tail drag loads under nonvacuum conditions). This provided the cancellation of the inertial reactive loads measured by the forward strain beam.

The oscillator controls were then adjusted so that, at the same frequency of about 8 cps, a pure rotational motion was set up with the $\underline{D}_F$ signal indicating less than 1/4 g and the $\underline{D}_A + K_1 \underline{D}_F$ signal indicating 50 radians/sec.^{2}. The $\underline{M}_A + K_2 \underline{M}_F$ readout was then calibrated in counts/ft.lb. by ratioing it to the product of the F-104 model inertia in ft.lbs.sec.^{2} times the angular acceleration in radians/sec.^{2}, as indicated by $\underline{D}_A + K_1 \underline{D}_F$. (This calibration of $\underline{M}_A + K_2 \underline{M}_F$ was used to check that this signal had, in fact, been reduced to nearly zero during the adjustment of K_2 under pure plunging conditions.) A signal from $\underline{D}_A + K_1 \underline{D}_F$ was then subtracted from the $\underline{M}_A + K_2 \underline{M}_F$ signal in an amount $I_M^* (\underline{D}_A + K_1 \underline{D}_F)$ so that the $\underline{M}_A + K_2 \underline{M}_F$ readout was zero (to within the moment due to tail drag and virtual mass). This then provided the cancellation of the inertial reactive moments due to the angular acceleration of the F-104 model (see Figure 6).

These calibrations of the $\underline{M}_F$ and $\underline{M}_A + K_2 \underline{M}_F$ channels and the inertia canceling effectiveness of the dummy model were then checked for several different combinations of linear and angular accelerations and several frequencies.

Test signals again provided the calibrations of each of the readout channels in terms of counts of readout/peak volt of input signal which enabled the conversion of the calibrations from counts/unit measured to volts/unit measured. With excitation voltage to the strain-gage bridges of 5.27 volts, the sensitivities were determined to be 0.0175 volts/lb. for the $\underline{M}_F$ channel and 0.1144 volts/ft.lb. for the $\underline{M}_A + K_2 \underline{M}_F$ channel and constant with frequency over the operating range.

The excitation voltage to all the strain-gage bridges was 5.27 volts and each channel had an amplifier with a gain of 2,000. The $\underline{M}_A + K_2 \underline{M}_F$ and the $\underline{D}_A + K_1 \underline{D}_F$ channels had additional amplifiers with gains of four. Taking these facts into account, the sensitivity of each of the strain-gage beams in terms of microvolts/lb. of load/volt of excitation were determined to be as follows:

$\underline{M}_F$	1.66
$\underline{M}_A + K_2 \underline{M}_F$	1.80
$\underline{D}_A$	1.40
$\underline{D}_A + K_1 \underline{D}_F$	1.49

Henceforth in this report, the four readout channels will be designated by the same symbols introduced in Part I of this report.

$\underline{M}_F$ will be replaced by $\underline{(F)}$ representing the aerodynamic normal force,

$\underline{M}_A + K_2 \underline{M}_F$ will be replaced by $\underline{(M)}$ representing the aerodynamic pitching moment,

$\underline{D}_A$ will be replaced by $\underline{(A)}$ representing the angular acceleration, and

$\underline{D}_A + K_1 \underline{D}_F$ will be replaced by $\underline{(L)}$ representing the linear acceleration.

SECTION 5

THE WIND-TUNNEL TEST PROGRAM

For the wind-tunnel tests, the F-104 model mounted on the dynamic testing sting and cart were installed in CAL's 8-Ft. Variable-Density Transonic Wind Tunnel, as shown in Figure 7.

The first run in the wind tunnel was performed under wind-off conditions and constituted a check at reduced density of the calibration of the F-104 model balance and of the cancellation of the inertial reactive loads. With the sphere evacuated to a density of about 1/6 atmosphere, the oscillator controls were adjusted to produce a pure plunging motion having about 10 g's of vertical acceleration and less than 1/4 radian/sec.^{2} of angular acceleration. Refer to Figure 6. The quantity K_2 was adjusted until the pitching moment was zero. Then W_M^* was adjusted until the normal force readout was zero. With W_M^* set to zero, a check of the calibration of the (F) readout was made by ratioing it to the weight of the model (12.8 lbs.) times the g's of vertical acceleration.

The oscillator controls were then adjusted to provide a pure rotation at about 50 radians/sec.^{2} of angular acceleration and less than 1/4 g of vertical acceleration. Again with reference to Figure 6, the quantity I_M^* was adjusted until the pitching moment was zero. With the quantity I_M^* set to zero, a check of the calibration of the (M) readout was made by ratioing it to the product of the model inertia (0.402 ft.lbs. sec.^{2}) times the angular acceleration in radians/sec.^{2}.

The oscillator controls were again readjusted to a pure plunge condition of about 10 g's and less than 1/4 radian/sec.^{2}. With all aspects of signal mixing in their final configuration, the normal force and pitching moment were monitored as the density was increased from 1/6 atmosphere to 1/4 atmosphere, then 1/2 atmosphere, and, finally, 1 atmosphere.

These tests provided a check of the previous calibrations of the F-104 model balance and also demonstrated that (1) by adjusting K_2, the pitching moment could be corrected for displaced model c.g. to within 0.1 ft.lbs. at 10 g's of vertical acceleration; (2) the normal force due to inertial reaction during plunging motion at 10 g's of vertical acceleration could be canceled with W_M^* to within 4 lbs. (out of a total of 128 lbs. of normal force). This could not have been improved upon significantly, since the remainder was mostly in quadrature with the linear acceleration. (3) The pitching moment due to inertial reaction during pure rotation at about 50 radians/sec.^{2} could be canceled with I_M^* to within 0.6 ft.lbs. (out of a total of about 20 ft.lbs. of pitching moment).

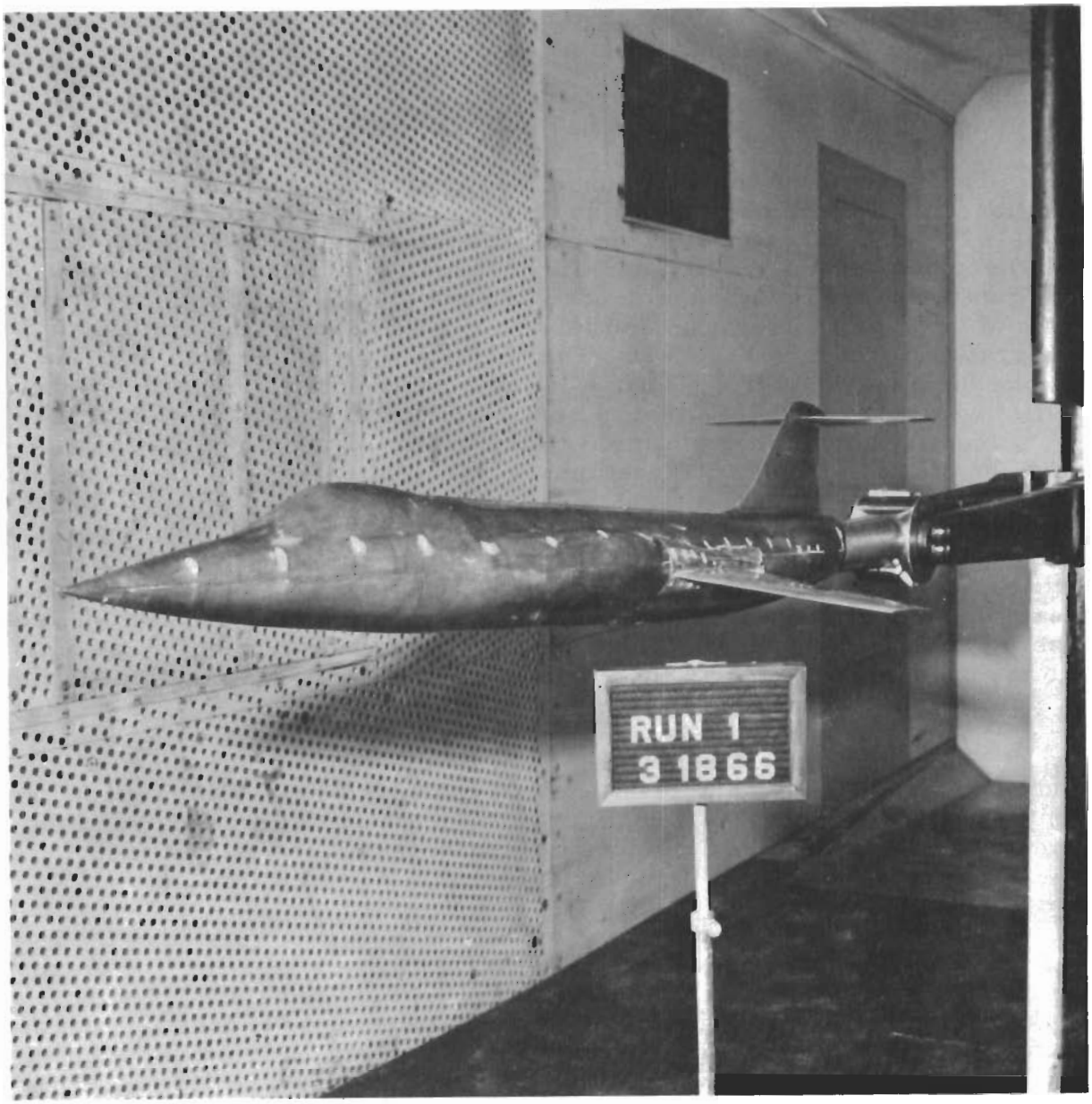

Figure 7 F-104 MODEL READY FOR DYNAMIC TESTS IN CAL'S 8-FT TRANSONIC WIND TUNNEL

As a point of interest, a reinterpretation of the potentiometer settings corresponding to W_M^* , I_M^* , K_1 and K_2 indicates the following:

(1) The potentiometer setting required to cancel the normal force due to inertial reactive load during pure plunging (W_M^* = 1.113 volts/volt) indicated a model weight of 12.3 lbs. as compared to the actual weight of 12.8 lbs.

(2) The potentiometer setting required to cancel the pitching moment due to inertial reactive loads during pure rotation (I_M^* = 1.180 volts/volt) indicated a moment of inertia for the model of 0.403 ft. lbs. sec.^{2} as compared to the previously measured 0.402 ft. lbs. sec.^{2} .

(3) The potentiometer setting required to zero the readout corresponding to angular acceleration during pure plunging (K_1 = 0.0176 volts/volt) indicated that the center of gravity of the dummy model was displaced aft about 0.03 in.

(4) The potentiometer setting required to null the pitching moment readout under near-vacuum conditions during pure plunging motion (K_2 = 0.006 volts/volt) indicated that the F-104 model center of gravity was displaced aft about 0.01 in.

The second run was the first series of wind-on tests but was performed with the mechanical oscillator locked and constituted a relatively ordinary static wind-tunnel test. This series served two purposes — first, to obtain an indication of the static out-of-trim pitching moment at the angle of attack corresponding to the mean angle about which oscillatory tests would be performed, and second, to obtain an indication of noise levels to be encountered at the proposed combinations of dynamic pressures and Mach numbers. For these purposes, the angular acceleration and pitching moment readouts were monitored on direct-recording equipment. The results of these tests indicated a significantly larger out-of-trim moment than had been anticipated.

In designing the forward sting support for this F-104 model, an estimate of the static trim angle had been obtained on the basis of flight test data taken from Reference 2. These data had indicated that the static trim angle might be as large as 4.2°. A compromise for Mach numbers up to 1.2 between these data and results of static wind-tunnel tests [3] was the choice of a 3° trim angle of attack as a basis for the design of the forward sting. The measurements made of the pitching moment during the second run are shown in Figure 8 in comparison with static wind-tunnel test data taken from Reference 3. This shows that the static angle of attack achieved was apparently between 3° and 4° but that a much better value would have been about 1-1/2°. At the higher Mach numbers, the static moment indicated in Figure 8 constituted more than half the capacity of the F-104 model moment balance. The testing capabilities were further limited by the maximum allowable normal force on the balance. The static lift force

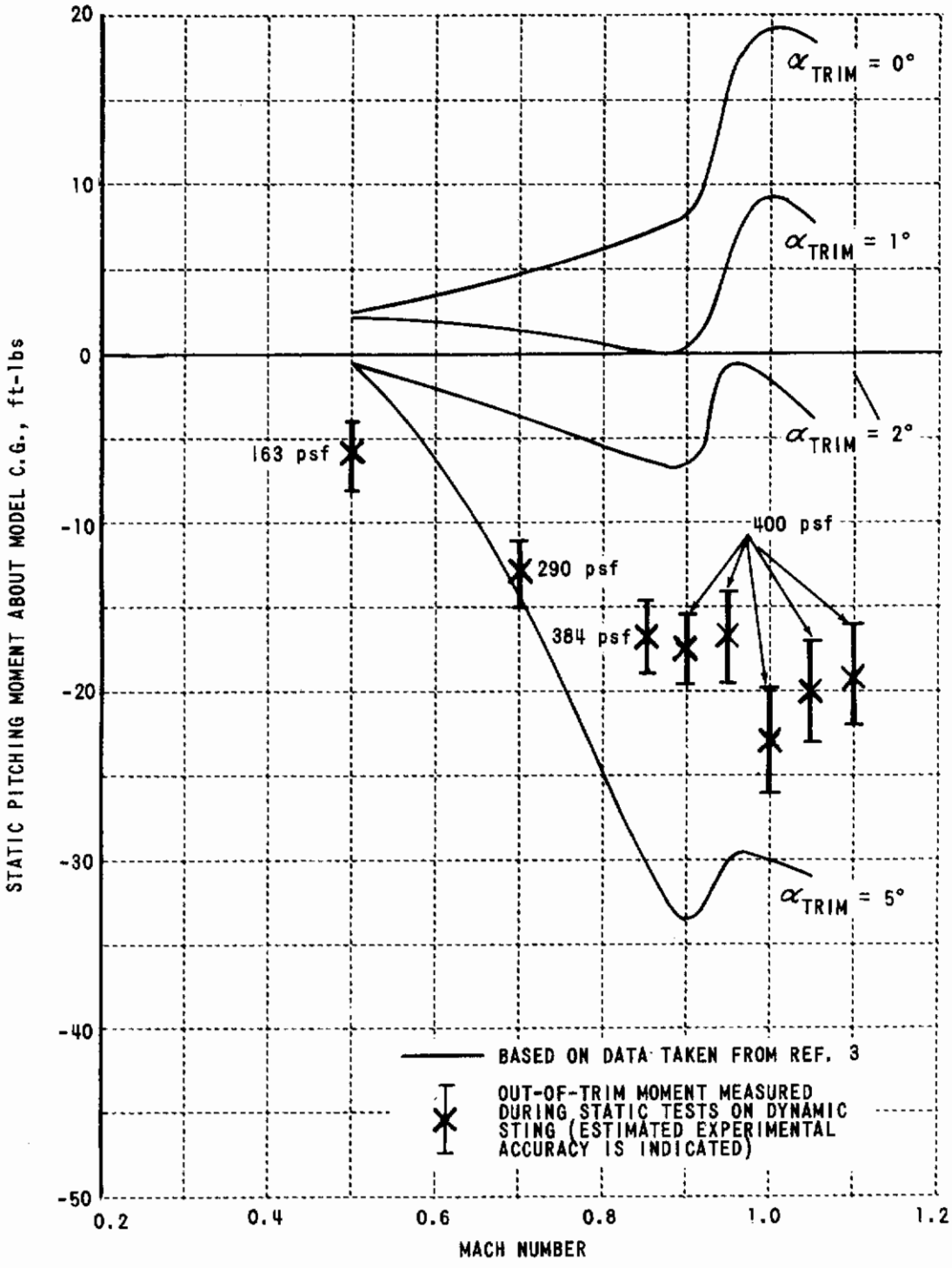

Figure 8 STATIC PITCHING MOMENT ABOUT THE MODEL C.G. VS. MACH NUMBER

under the conditions corresponding to those of the data of Figure 8 could have exceeded 200 lbs. or about half the capacity of the normal force beams. The oscillograph records of the pitching moment and the angular acceleration showed also that the noise levels became higher than desirable at the higher Mach numbers during the tests at a dynamic pressure of 400 psf. Consequently, in light of all of these results, it was decided to limit the model motions to 10 g's and 50 radians/sec.^{2} and to conduct all the dynamic tests at a dynamic pressure of 300 psf.

During the dynamic tests, the wind-off (i. e. $M=0$) data were taken under tunnel density conditions corresponding to about 1/2 atmosphere. The wind-on data were all taken at a dynamic pressure of about 300 psf corresponding to a range of Reynolds number from about 1. 6 to 2. 0 x 10^6/ft. The following tests were conducted:

Run 3

Pure rotation tests at 7. 15 cps (τ = 0. 1400) at an angular acceleration of about 45 radians/sec.^{2} and less than 1/4 g of vertical acceleration. Data were obtained at Mach numbers of 0, 0. 70, 0. 85, 0. 90, 0. 95, 1. 00, 1. 05, and 1. 10.

Run 4

Pure rotation at 3. 92 cps (τ = 0. 2550) at an angular acceleration of about 25 radians/sec.^{2} and less than 1/4 g of vertical acceleration. Data were obtained at Mach numbers of 0, 0. 90, 0. 95, 1. 00, 1. 05, and 1. 10.

Run 5

Pure plunge at 3. 92 cps (τ = 0. 2550) at a vertical acceleration of about 6 g's and less than 1/8 radian/sec.^{2} of angular acceleration. Data were obtained at Mach numbers of 0, 0. 90, 0. 95, 1. 00, 1. 05, and 1. 10.

Run 6

Pure plunge at 7. 15 cps (τ = 0. 1400) at a vertical acceleration of about 10 g's and less than 1/4 radian/sec.^{2} of angular acceleration. Data were obtained at Mach numbers of 0, 0. 70, 0. 85, 0. 90, 0. 95, 1. 00, 1. 05, and 1. 10.

Run 7

Pure rotation at 10 cps (τ = 0. 1000) at an angular acceleration of about 44 radians/sec.^{2} and less than 1/4 g of vertical acceleration. Data were obtained at Mach numbers of 0, 0. 95, 1. 00, and 1. 05.

Run 8

Pure pitch at 7.15 cps (τ = 0.1400) at a vertical acceleration of 10 g's $\pm$1/4 g. The angular acceleration required at each Mach number to maintain a constant angle of attack was adjusted to within $\pm$0.4 radian/sec.^{2}. The motion was adjusted so that the phase of the angular acceleration lagged the linear acceleration by 90° $\pm$1/2°. Data were taken at M = 0 with an angular acceleration of 13.1 radians/sec.^{2}, at M = 0.95 where U was 1015 fps and the required angular acceleration was 14.3 radians/sec.^{2}; at M = 1.00 where U was 1066 fps and the required angular acceleration was 13.6 radians/sec.^{2}, and at M = 1.05 where U was 1108 fps and the required angular acceleration was 13.1 radians/sec.^{2}.

Run 9

Run 9 was a single test point taken at Mach number of 1.2 of pure rotation at 3.92 cps with about 25 radians/sec.^{2} of angular acceleration and less than 1/4 g of linear acceleration.

SECTION 6

DATA REDUCTION AND ANALYSES

The data were reduced by procedures described in detail in Part I of this report [1]. Results in the form of lift and moment derivatives are presented in Tables II, III and IV. In Table II are the results of the rotation tests from which measurements could be made of the derivatives C_{L_α}, $C_{L_{\dot\alpha}} + C_{L_{\dot\theta}}$, C_{m_α}, and $C_{m_{\dot\alpha}} + C_{m_{\dot\theta}}$. In general, the dynamic measurements of the static derivatives C_{L_α} and C_{m_α} at all three frequencies are in excellent agreement (in general, within 10%). The measurements of the rotary damping derivatives $C_{m_{\dot\alpha}} + C_{m_{\dot\theta}}$ at 7 cps and 10 cps agree within about 10%. The corresponding quantities measured at 4 cps differ from these by about 30%, however. The spread in all the measurements of $C_{L_{\dot\alpha}} + C_{L_{\dot\theta}}$ is about $\pm 20\%$. A significant consideration with regard to these differences is that any of them can be accounted for by about 1° change in the measured phase angle between the force or moment vector and the motion vector.

Table III presents the results of plunge tests made at about 4 cps and 7 cps. Again, dynamic measures of the static derivatives C_{L_α} and C_{m_α} are in excellent agreement and, also, compare very well with the corresponding measurements made in rotation tests. However, the measurements of the lift and moment due to rate of change of angle of attack $C_{L_{\dot\alpha}}$ and $C_{m_{\dot\alpha}}$ made at 3.92 cps are not in satisfactory agreement with those made at 7.15 cps.

Table IV presents the results of three cases of pure pitching motion at 7.15 cps. These tests provided measures of the lift and pitching moment due to pitch rate, $C_{L_{\dot\theta}}$ and $C_{m_{\dot\theta}}$. Shown also are the sums of these derivatives with the associated dynamic derivatives measured during plunge tests and the comparison of these sums with the total dynamic derivatives measured during the pure rotation tests. The agreement in the moment derivatives is, obviously, excellent and even the lift derivatives are in surprisingly good agreement.

The results of the pitching moment measurements made during these tests are also summarized in Figure 9. Very satisfactory results were obtained in all cases, with the exception of tests at 4 cps. No explanation can be given for the discrepancies at 4 cps, except to point out once again that the measures of the dynamic derivatives at low frequencies are extremely sensitive to errors in phase measurement.

The results of these tests are compared with measurements made on similar models in other facilities in Figures 10, 11 and 12. Data are taken from References 3, 4 and 5, and dimensional comparisons of the NASA models with the Air Force model are presented in Table I. The geometry and center-of-gravity location of the Air Force model were quite close to that of the full-scale F-104 aircraft. The NASA wind-tunnel models all had c.g. locations, moment centers, and oscillation centers at 25% of the mean aerodynamic chord, rather than at 16.6% chord as did the Air Force model.

TABLE II
ROTATION TEST RESULTS

AT 3.92 cps (RUN #4 AND #9)

ANGULAR ACCELERATION $\doteq \pm$ 25 RAD/SEC^2
ANGULAR VELOCITY $\doteq \pm$ 1.02 RAD/SEC
ANGULAR DISPLACEMENT $\doteq \pm$ 2.4 DEG

M	C_{L_α}	$C_{L_{\dot\alpha}} + C_{L_{\dot\theta}}$	C_{m_α}	$C_{m_{\dot\alpha}} + C_{m_{\dot\theta}}$
0.90	+0.068	+0.477	-0.014	-0.438
0.95	+0.074	+0.476	-0.024	-0.555
1.00	+0.070	+0.632	-0.028	-0.556
1.05	+0.068	+0.294	-0.027	-0.670
1.10	+0.065	+0.374	-0.032	-0.529
1.20	+0.062	+0.648	-0.032	-0.788

AT 7.15 cps (RUN #3)

ANGULAR ACCELERATION $\doteq \pm$ 45 RAD/SEC^2
ANGULAR VELOCITY $\doteq \pm$ 1 RAD/SEC
ANGULAR DISPLACEMENT $\doteq \pm$ 1.3 DEG

M	C_{L_α}	$C_{L_{\dot\alpha}} + C_{L_{\dot\theta}}$	C_{m_α}	$C_{m_{\dot\alpha}} + C_{m_{\dot\theta}}$
0.70	+0.055	+0.366	-0.010	-0.245
0.85	+0.060	+0.472	-0.009	-0.299
0.90	+0.065	+0.509	-0.011	-0.358
0.95	+0.070	+0.456	-0.022	-0.450
1.00	+0.068	+0.509	-0.026	-0.426
1.05	+0.065	+0.468	-0.026	-0.591
1.10	+0.062	+0.515	-0.030	-0.432

AT 10.00 cps (RUN #7)

ANGULAR ACCELERATION $\doteq \pm$ 44 RAD/SEC^2
ANGULAR VELOCITY $\doteq \pm$ 0.7 RAD/SEC
ANGULAR DISPLACEMENT $\doteq \pm$ 0.6 DEG

M	C_{L_α}	$C_{L_{\dot\alpha}} + C_{L_{\dot\theta}}$	C_{m_α}	$C_{m_{\dot\alpha}} + C_{m_{\dot\theta}}$
0.95	+0.066	+0.366	-0.024	-0.457
1.00	+0.065	+0.432	-0.029	-0.383
1.05	+0.061	+0.400	-0.031	-0.563

TABLE III
PLUNGE TEST RESULTS

AT 3.92 cps (RUN #5)

VERTICAL ACCELERATION $\doteq \pm 6.3$ g's $= 205$ fps^2

VERTICAL VELOCITY $\doteq \pm 8.33$ fps

M	U	α(deg)	$\dot{\alpha}$(deg/sec)	C_{L_α}	$C_{L_{\dot{\alpha}}}$	C_{m_α}	$C_{m_{\dot{\alpha}}}$
0.90	971.8	0.49	12.2	+0.073	-2.18	-0.014	+0.027
0.95	1019.5	0.47	11.6	+0.081	-2.33	-0.027	+0.538
1.00	1071.9	0.45	11.0	+0.073	-2.08	-0.029	+0.487
1.05	1112.1	0.43	10.6	+0.069	-1.65	-0.027	+0.349
1.10	1138.6	0.42	10.3	+0.068	-1.72	-0.027	-0.591

AT 7.15 cps (RUN #6)

VERTICAL ACCELERATION $\doteq \pm 10.45$ g's $= 336$ fps^2

VERTICAL VELOCITY $\doteq \pm 7.5$ fps

M	U	α(deg)	$\dot{\alpha}$(deg/sec)	C_{L_α}	$C_{L_{\dot{\alpha}}}$	C_{m_α}	$C_{m_{\dot{\alpha}}}$
0.70	774.8	0.55	24.8	+0.053	-0.48	-0.011	-0.012
0.85	923.1	0.47	20.9	+0.060	-0.56	-0.011	-0.109
0.90	970.0	0.44	19.9	+0.065	-0.46	-0.013	-0.069
0.95	1015.9	0.42	19.0	+0.071	-0.36	-0.023	+0.045
1.00	1066.3	0.40	18.1	+0.066	-0.05	-0.026	+0.151
1.05	1108.2	0.39	17.4	+0.066	+0.03	-0.026	+0.070
1.10	1148.8	0.38	16.8	+0.065	+0.12	-0.025	-0.335

TABLE IV
PITCH TEST RESULTS

AT 7.15 cps (RUN #8)

PITCH RATE $\doteq \pm 0.3$ (rad/sec)

PITCH DISPLACEMENT $\doteq \pm 0.0067$ rad $= \pm 0.38$ deg

M	$C_{L_{\dot{\theta}}}$	$C_{m_{\dot{\theta}}}$	PLUNGE + PITCH		ROTATION	
			$C_{L_{\dot{\alpha}}} + C_{L_{\dot{\theta}}}$	$C_{m_{\dot{\alpha}}} + C_{m_{\dot{\theta}}}$	$C_{L_{\dot{\alpha}}} + C_{L_{\dot{\theta}}}$	$C_{m_{\dot{\alpha}}} + C_{m_{\dot{\theta}}}$
0.95	+0.560	-0.488	+0.200	-0.443	+0.456	-0.450
1.00	+0.439	-0.577	+0.389	-0.426	+0.509	-0.426
1.05	+0.718	-0.651	+0.748	-0.581	+0.468	-0.591

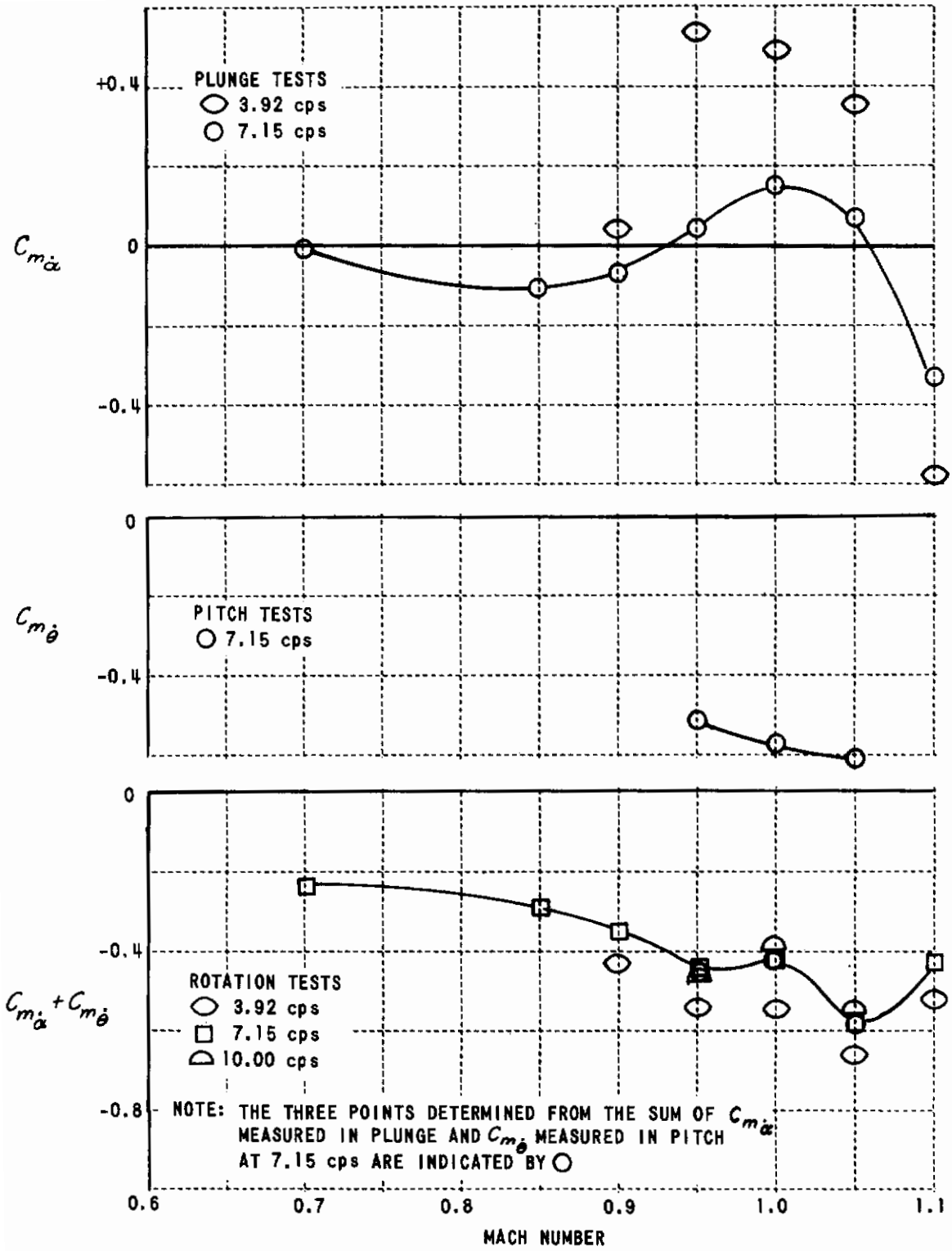

Figure 9 DYNAMIC PITCHING MOMENT DERIVATIVES VS. MACH NUMBER

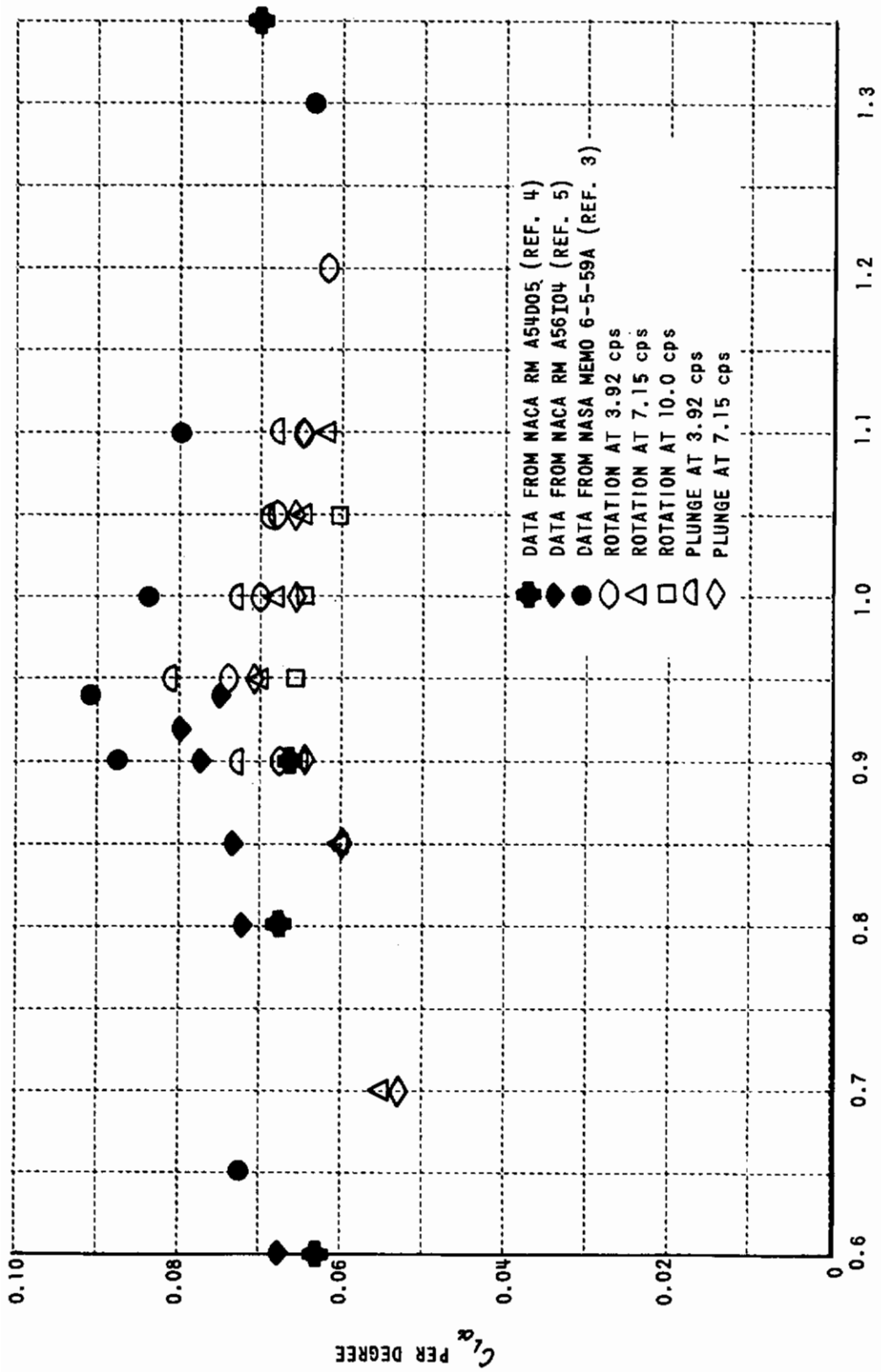

Figure 10 LIFT CURVE SLOPE VS. MACH NUMBER

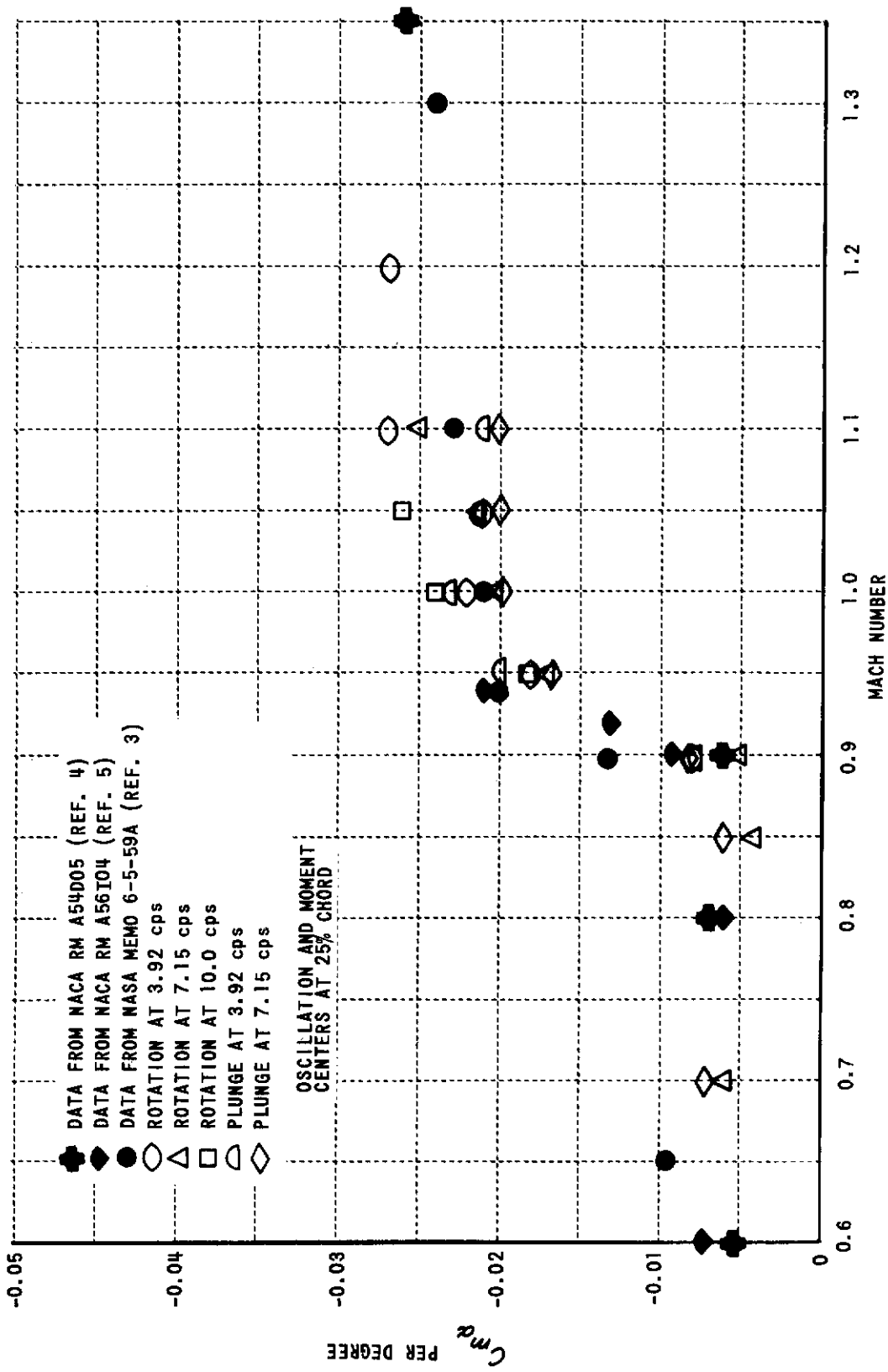

Figure 11 MOMENT CURVE SLOPE VS. MACH NUMBER

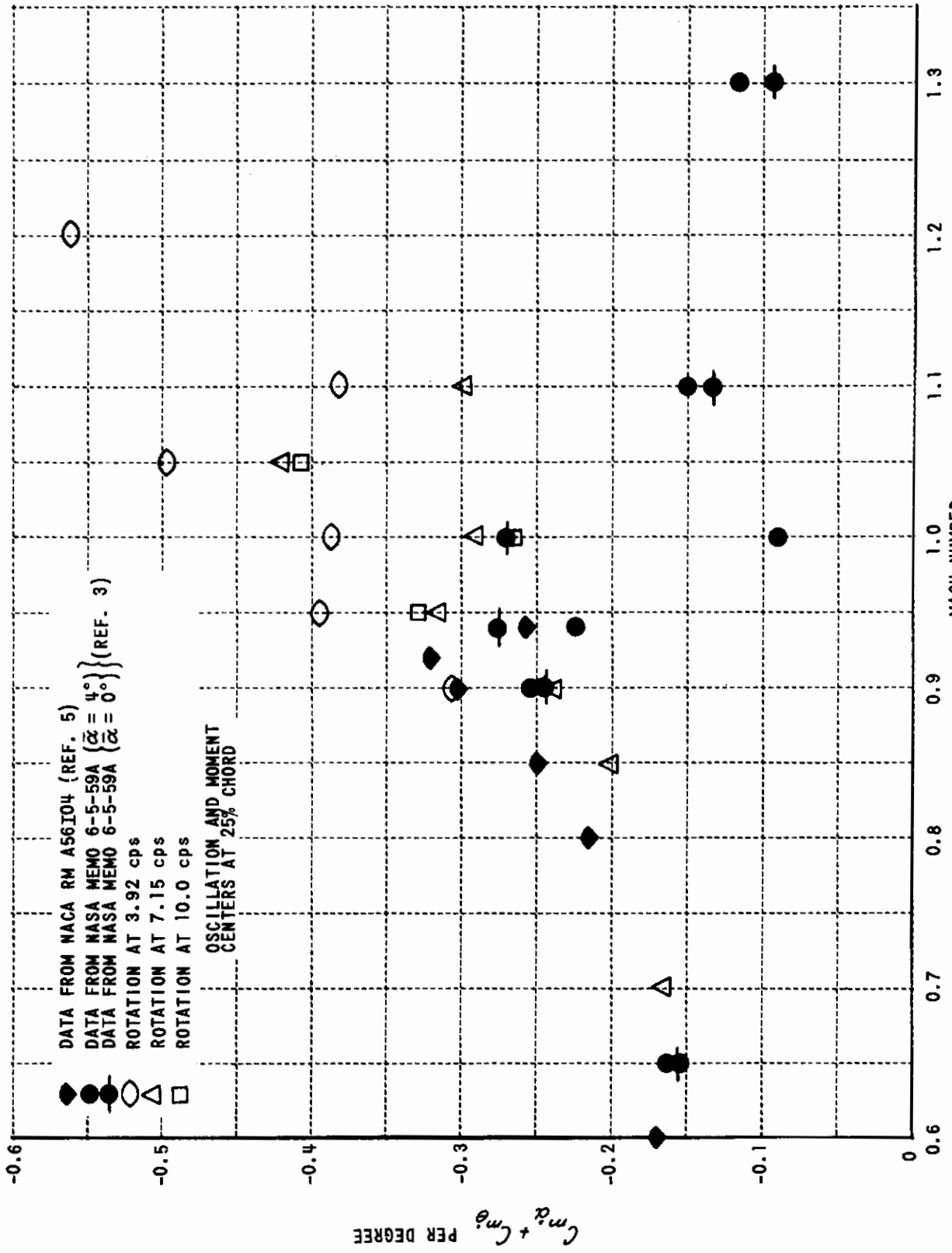

Figure 12 ROTARY DAMPING DERIVATIVE VS. MACH NUMBER

The aerodynamic derivatives measured during the tests reported herein and presented in Tables II, III and IV and in Figure 9 were, therefore, transformed from an oscillation and moment center at 16.6% of the mean aerodynamic chord to an oscillation center at 25% chord for comparison with these other data. To accomplish this transformation, equations from Reference 3 were used. If the oscillation center designated "1" is the axis about which the derivatives were measured, they can be transferred to another oscillation center designated "2" which is $\bar{x}$ ft. forward of position "1" by the following equations:

$$C_{L_{\alpha_2}} = C_{L_{\alpha_1}}$$

$$(C_{L_{\dot{\alpha}}} + C_{L_{\dot{\theta}}})_2 = (C_{L_{\dot{\alpha}}} + C_{L_{\dot{\theta}}})_1 + C_{L_\alpha}\left(\frac{2\bar{x}}{c}\right)$$

$$C_{m_{\alpha_2}} = C_{m_{\alpha_1}} - C_{L_\alpha}\left(\frac{\bar{x}}{c}\right)$$

$$(C_{m_{\dot{\alpha}}} + C_{m_{\dot{\theta}}})_2 = (C_{m_{\dot{\alpha}}} + C_{m_{\dot{\theta}}})_1 - (C_{L_{\dot{\alpha}}} + C_{L_{\dot{\theta}}})_1\left(\frac{\bar{x}}{c}\right) + C_{m_{\alpha_1}}\left(\frac{2\bar{x}}{c}\right) - 2C_{L_\alpha}\left(\frac{\bar{x}}{c}\right)^2$$

In addition to this transformation of the moment center, the data were also adjusted for differences in scaled tail lengths. As shown in Table I, the body length and (correspondingly) the tail length of the Air Force model are about 10% greater than the NASA models when they are comparably scaled.

The dynamic measures of the static derivatives C_{L_α} and C_{m_α} are in good agreement with static and dynamic measurements of these quantities taken from References 3, 4 and 5 as shown in Figures 10 and 11. Measurements of the total rotary damping derivative $C_{m_{\dot{\alpha}}} + C_{m_{\dot{\theta}}}$ taken from References 3 and 5 are shown in Figure 12. The data from Reference 5 were all taken about a mean angle of attack of about 4°. The corresponding data from Reference 3 for a mean angle of attack of 4° indicate a sharp decrease in the magnitude of the damping at $M = 1.0$. Although a decrease at $M = 1.0$ is also indicated by the present data, it is not nearly as large as that of the data of Reference 3. As a point of interest in this regard, the data for a mean angle of attack of 0° were also taken from Reference 3 and are shown on Figure 12 for comparison. There is no decrease at all in the damping in a narrow region about $M = 1$ in this case as there was for $\bar{\alpha} = 4°$; although a decrease is evident at M = 1.1 .

SECTION 7

CONCLUDING REMARKS

In comparison with the tests of the F-80 model reported in Part I [1], dynamic tests of the F-104 model were severely limited by (1) the increased weight of the model (by over 40%), (2) the lower allowable load limits on both the normal force and moment balances, and (3) the unfortunate poor estimate of the trim angle of attack. Nevertheless, the results were, in general, quite satisfactory particularly in light of these limitations.

The dummy-model approach for measurement of the model motion and for cancellation of the inertial reactive loads worked very well. In comparison with the force and motion sensors used in the F-80 model, there is an operational advantage to having four identical transducers, none of which introduce significant phase shift over the operating frequency range (that is, where both the forces and the motion are measured by strain-gage beams). This in itself is not sufficient advantage for the dummy-model approach in view of the facts that the model is considerably more difficult to build and the load at the end of the sting is nearly doubled. It is recommended, therefore, that linear and angular accelerometers be used for motion sensors in future models as they were in the F-80 model tests [1].

In view of the load limitations on the F-104 model, only pure rotation tests and measurements of the total rotary damping derivative had been anticipated. The overall accuracy of the dynamic testing system was good enough, however, to enable satisfactory measurements to be made during pure plunging and pure pitching tests, even though the linear accelerations had to be limited to 10 g's. In retrospect, it is regrettable that time did not permit the performance of additional pitching tests at other Mach numbers and both plunging and pitching tests at other frequencies.

It is apparent that the rate-dependent aerodynamic terms cannot be measured accurately at low oscillation frequencies. For a constant amplitude of oscillation, these terms decrease linearly with decreasing frequency. The phase angle between the force or moment vector and the motion vector cannot be measured with sufficient accuracy to enable an accurate measure of the small rate-dependent component at low frequencies. Dynamic tests should be performed at the highest possible frequencies consistent with reasonable values for the reduced frequencies.

The modifications to the dynamic testing system which had been made since completion of the F-80 model tests produced substantial improvement in its operation. Indicative of this is the fact that the entire series of dynamic tests with the F-104 model consisting of 37 data points was completed in an elapsed time of about 5-1/2 hours, whereas the 33 dynamic test points with the F-80 model required an elapsed time of just over 8 hours.

REFERENCES

1. Statler, I. C., Tufts, O. B. and Hirtreiter, W. J., The Development and Evaluation of the CAL/Air Force Dynamic Wind-Tunnel Testing System, Part I - Description and Dynamic Tests of an F-80 Model, AFFDL-TR-66-153, Part I (to be published)

2. Andrews, W. H. and Rediess, H. A., Flight-Determined Stability and Control Derivatives of a Supersonic Airplane with a Low-Aspect-Ratio Unswept Wing and a Tee-Tail, NASA Memo 2-2-59H, April 1959.

3. Lessing, H. C. and Butler, J. K., Wind-Tunnel Investigation at Subsonic and Supersonic Speeds of the Static and Dynamic Stability Derivatives of an Airplane Model with an Unswept Wing and a High Horizontal Tail, NASA Memo 6-5-59A, June 1959.

4. Smith, W. G., Wind-Tunnel Investigation at Subsonic and Supersonic Speeds of a Fighter Model Employing a Low-Aspect-Ratio Unswept Wing and a Horizontal Tail Mounted Well Above the Wing Plane — Longitudinal Stability and Control, NACA Research Memorandum A54D05, November 1954.

5. Buell, D. A., Reed, V. D. and Lopez, A. E., The Static and Dynamic-Rotary Stability Derivatives at Subsonic Speeds of an Airplane Model with an Unswept Wing and a High Horizontal Tail, NACA Research Memorandum A56I04, December 1956.

UNCLASSIFIED
Security Classification

DOCUMENT CONTROL DATA - R&D
(Security classification of title, body of abstract and indexing annotation must be entered when the overall report is classified)

1. ORIGINATING ACTIVITY (Corporate author)
Cornell Aeronautical Laboratory, Inc.
Buffalo, New York 14221

2a. REPORT SECURITY CLASSIFICATION
UNCLASSIFIED

2b. GROUP

3. REPORT TITLE
The Development and Evaluation of the CAL/Air Force Dynamic Wind-Tunnel Testing System, Part II - Dynamic Tests of an F-104 Model

4. DESCRIPTIVE NOTES (Type of report and inclusive dates)
Final Report, March 1961 - August 1966

5. AUTHOR(S) (Last name, first name, initial)
Statler, Irving C.

6. REPORT DATE	7a. TOTAL NO. OF PAGES	7b. NO. OF REFS
February 1967	40	5

8a. CONTRACT OR GRANT NO.	9a. ORIGINATOR'S REPORT NUMBER(S)
AF 33(616)-8034	
b. PROJECT NO. 8219, Task No. 821902	
c.	9b. OTHER REPORT NO(S) (Any other numbers that may be assigned this report)
d.	AFFDL-TR-66-153, Part II

10. AVAILABILITY/LIMITATION NOTICES
Distribution of this document is unlimited.

11. SUPPLEMENTARY NOTES	12. SPONSORING MILITARY ACTIVITY
Part I of this report discusses dynamic tests of an F-80 model.	Air Force Flight Dynamics Laboratory Research and Technology Division Wright-Patterson Air Force Base, Ohio

13. ABSTRACT

The development of a new technique for dynamic testing in wind tunnels and evaluation tests of the system with an F-80 model were described in Part I of this report. Although those tests adequately demonstrated the unusual capabilities of this dynamic testing system, the F-80 model was limited to subsonic speeds. This part of the report (Part II) describes an additional series of evaluation tests that were performed with a model of an F-104 airplane. The model had been designed and fabricated by the Air Force Flight Dynamics Laboratory and incorporated an unusual force and motion sensing system utilizing an internal dummy model with duplicate mass, inertia, and c.g. location. Longitudinal dynamic tests were performed with this model up through the transonic speed range. The results are evaluated with respect to the operation of the dynamic testing system and to the performance of the dummy model for measuring motion and canceling inertial loads.

DD FORM 1 JAN 64 1473

UNCLASSIFIED
Security Classification

UNCLASSIFIED
Security Classification

14. KEY WORDS	LINK A		LINK B		LINK C	
	ROLE	WT	ROLE	WT	ROLE	WT
Dynamic Wind-Tunnel Testing Wind-Tunnel Testing Dynamic Stability Rotary Damping Derivatives Forced Oscillation Tests F-104						

INSTRUCTIONS

1. ORIGINATING ACTIVITY: Enter the name and address of the contractor, subcontractor, grantee, Department of Defense activity or other organization *(corporate author)* issuing the report.

2*a*. REPORT SECURITY CLASSIFICATION: Enter the overall security classification of the report. Indicate whether "Restricted Data" is included. Marking is to be in accordance with appropriate security regulations.

2*b*. GROUP: Automatic downgrading is specified in DoD Directive 5200.10 and Armed Forces Industrial Manual. Enter the group number. Also, when applicable, show that optional markings have been used for Group 3 and Group 4 as authorized.

3. REPORT TITLE: Enter the complete report title in all capital letters. Titles in all cases should be unclassified. If a meaningful title cannot be selected without classification, show title classification in all capitals in parenthesis immediately following the title.

4. DESCRIPTIVE NOTES: If appropriate, enter the type of report, e.g., interim, progress, summary, annual, or final. Give the inclusive dates when a specific reporting period is covered.

5. AUTHOR(S): Enter the name(s) of author(s) as shown on or in the report. Enter last name, first name, middle initial. If military, show rank and branch of service. The name of the principal author is an absolute minimum requirement.

6. REPORT DATE: Enter the date of the report as day, month, year; or month, year. If more than one date appears on the report, use date of publication.

7*a*. TOTAL NUMBER OF PAGES: The total page count should follow normal pagination procedures, i.e., enter the number of pages containing information.

7*b*. NUMBER OF REFERENCES: Enter the total number of references cited in the report.

8*a*. CONTRACT OR GRANT NUMBER: If appropriate, enter the applicable number of the contract or grant under which the report was written.

8*b*, 8*c*, & 8*d*. PROJECT NUMBER: Enter the appropriate military department identification, such as project number, subproject number, system numbers, task number, etc.

9*a*. ORIGINATOR'S REPORT NUMBER(S): Enter the official report number by which the document will be identified and controlled by the originating activity. This number must be unique to this report.

9*b*. OTHER REPORT NUMBER(S): If the report has been assigned any other report numbers *(either by the originator or by the sponsor)*, also enter this number(s).

10. AVAILABILITY/LIMITATION NOTICES: Enter any limitations on further dissemination of the report, other than those imposed by security classification, using standard statements such as:

(1) "Qualified requesters may obtain copies of this report from DDC."

(2) "Foreign announcement and dissemination of this report by DDC is not authorized."

(3) "U. S. Government agencies may obtain copies of this report directly from DDC. Other qualified DDC users shall request through _____."

(4) "U. S. military agencies may obtain copies of this report directly from DDC. Other qualified users shall request through _____."

(5) "All distribution of this report is controlled. Qualified DDC users shall request through _____."

If the report has been furnished to the Office of Technical Services, Department of Commerce, for sale to the public, indicate this fact and enter the price, if known.

11. SUPPLEMENTARY NOTES: Use for additional explanatory notes.

12. SPONSORING MILITARY ACTIVITY: Enter the name of the departmental project office or laboratory sponsoring *(paying for)* the research and development. Include address.

13. ABSTRACT: Enter an abstract giving a brief and factual summary of the document indicative of the report, even though it may also appear elsewhere in the body of the technical report. If additional space is required, a continuation sheet shall be attached.

It is highly desirable that the abstract of classified reports be unclassified. Each paragraph of the abstract shall end with an indication of the military security classification of the information in the paragraph, represented as *(TS)*, *(S)*, *(C)*, or *(U)*.

There is no limitation on the length of the abstract. However, the suggested length is from 150 to 225 words.

14. KEY WORDS: Key words are technically meaningful terms or short phrases that characterize a report and may be used as index entries for cataloging the report. Key words must be selected so that no security classification is required. Identifiers, such as equipment model designation, trade name, military project code name, geographic location, may be used as key words but will be followed by an indication of technical context. The assignment of links, rules, and weights is optional.

UNCLASSIFIED
Security Classification